



Preparation of WO₃-modified TiO₂ thin film by peroxo sol–gel method and its photocatalytic activity in degradation of methylene blue

Jia-Ying Wu¹ · Yu-Wen Chen¹

Received: 14 July 2020 / Accepted: 30 July 2020 / Published online: 7 August 2020
© Springer Nature B.V. 2020

Abstract

A series of WO₃-modified TiO₂ sols with various WO₃ contents were synthesized by peroxo sol–gel method using H₂O₂ as the agent. The as-synthesized WO₃-TiO₂ sols were light yellow in color. The maximum amount of WO₃ which could be incorporated into the TiO₂ sol was 4 wt.%. The pH values of the as-prepared sols were near neutral. These sols were very stable even after 2 years in stock. The sols were used to coat on glass substrate. The XRD patterns and the SAED patterns indicated that the phase of TiO₂ was anatase. There were no characteristic XRD peaks of WO₃ in the WO₃-modified TiO₂ sol, possibly due to low WO₃ loading. The particles were rhombus shaped with the major axis and minor axis of 30–77 nm and 15–31 nm, respectively. WO₃ was incorporated into the surface structure of TiO₂ and modified the electronic state of Ti. The film coated onto glass substrate was very uniform, and the film thickness was ~ 160 nm. The XPS results exhibited that W existed as 5+ and 6+ oxidation states and Ti existed in Ti³⁺ and Ti⁴⁺. These four chemical states play a role of gathering the photogenerated holes and capturing the photogenerated electrons in the lower conduction band of WO₃, respectively. This can effectively enhance the separation rate of photogenerated electron–hole pairs and increase the photoactivity. WO₃/TiO₂ samples had high photocatalytic activity under UV light illumination to degrade methylene blue, because it had high OH and O²⁻ group contents.

Keywords WO₃-doped TiO₂ · Photocatalysis · Methylene blue destruction

✉ Yu-Wen Chen
ywchen@cc.ncu.edu.tw

¹ Department of Chemical and Materials Engineering, National Central University, Jhong-Li 32001, Taiwan

Introduction

TiO₂ has been well known to be the good material for degradation of dyes and anti-corrosion [1]. To enhance the photocatalytic activity of TiO₂, several strategies have been developed [1–9]. Adding WO₃ to TiO₂ can promote the activity under visible-light irradiation [9–14]. Ren et al. [15] have reported that TiCl₄ and Na₂WO₄ were applied as precursors to prepare TiO₂/WO₃ nanoparticles through microwave-assisted hydrothermal process. This composite catalyst showed greater photoactivity than TiO₂ in the degradation of Rhodamine B [15]. However, most of previous studies used powder form or sol in acidic solution [15–26]. The powder WO₃-TiO₂ cannot be used to coat on some substrates. The acidic sol is difficult to handle. There are many papers revealing some information about preparation WO₃-modified TiO₂ and their application on the photocatalytic reaction [27–47]. The effects of amount of WO₃ doping on the photocatalytic properties are not clear. Most of WO₃-TiO₂ sols reported in literature are acidic sols [43]. Some of them used conventional sol–gel method with alkoxide as the starting material. Alkoxide is easy to hydrolyze and cannot expose to air. None of them used peroxo sol–gel method to prepare WO₃-TiO₂ sol. In previous studies [47–54], one of the authors has used peroxo sol–gel method to prepare TiO₂-based sols. The sol was not acidic, and it has very high photocatalytic activity. The advantages of using peroxo sol–gel method to prepare TiO₂ sols were (1) transparent, (2) neutral (~pH 7) sol, (3) easy to coat on the substrate without using surfactant and strongly stick on the substrate, (4) formation of nanocrystallite in sol and no annealing is needed after coating, (5) stable, and (6) high photocatalytic activity.

In this study, WO₃ was used to modify TiO₂ since WO₃ can play a role of electron-accepting species. The objective of this study was to develop a method to prepare WO₃-TiO₂ sol. The peroxo sol–gel method was used in this study. We also tried to find the optimum doping amount of WO₃ and to investigate its applications on destruction of organic dyes.

Experimental

Synthesis of TiO₂ sol

The peroxo sol–gel method was used as those reported in the literature [42–50]. 5.88 ml TiCl₄ was slowly added into 300 ml 1 M HCl aqueous solution under constant-speed magnetic stirring and kept at 0 °C ice bath for 30 min. 1 M NH₄OH aqueous solution was then added dropwise to form white hydrated titanium oxide gel, Ti(OH)₄. The pH value of the gel was around 8.5. After aging for 30 min, Ti(OH)₄ gel was filtered and washed with distilled water several times to remove the residual chloride ion.

In order to prepare 1 wt.% TiO₂ sol, 10 g as-prepared gel was dispersed in 100 ml distilled water under magnetic stirring and ultrasonic vibration for 1 h

to form well-dispersed milky solution. An aqueous hydrogen peroxide solution (30 wt.% H₂O₂) was added dropwise into this milky solution under magnetic stirring for 2 h to get uniformly titanium peroxide solution with orange color. The molar ratio of TiO₂/H₂O₂ was 1:6. This solution was then heated up to 95 °C and kept at 95 °C for 12 h under magnetic stirring. The transparent TiO₂ sol with light yellow color was obtained.

Preparation of WO₃-modified TiO₂ sols

Sodium tungstate (Na₂WO₄) from Aldrich was used as the precursor of WO₃ in this study. The preparation method was the same as that of pure TiO₂ sol except that Na₂WO₄ was added in the last heating step. The weight ratios of WO₃/TiO₂ were 0.5:100, 1:100, 2:100 and 4:100, respectively. The detailed preparation procedure is shown in Fig. 1. TiCl₄ was dissolved in water to form Ti⁴⁺ ions. It was converted to Ti(OH)₄ gel after addition of NH₄OH. Ti(OH)₄ was converted to TiO₂ nanocrystals and Na₂WO₄ was converted to WO₃ nanocrystals by adding H₂O₂ and heating at 90–95 °C for a few hours. The catalyst was denoted as WT(x), where W means tungsten oxide, T means titanium oxide, and x stands for WO₃/TiO₂ weight ratio (%).

Preparation of WO₃-modified TiO₂ thin films

TiO₂ and WO₃-modified TiO₂ films were prepared by dip-coating method using the as-prepared pure TiO₂ and WO₃-modified TiO₂ sols. The method is the same as that reported in previous literature [48–53]. The substrate was soda-lime glass.

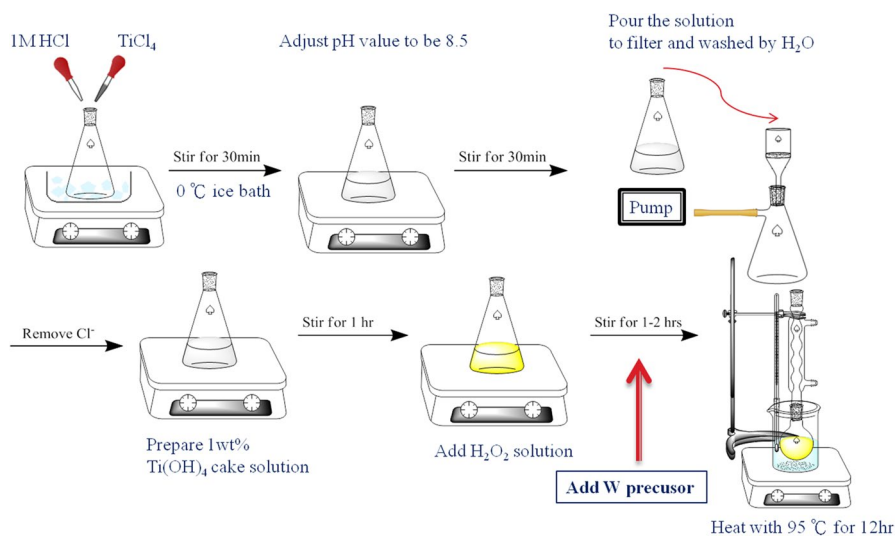


Fig. 1 The procedure of preparing WO₃-TiO₂ sol

The total coating surface area of these substrates was 40 cm². Before coating, the substrate was cleaned by washing solution, i.e., 1 M NH₄OH, and distilled water several times. The glass substrate was dried in an oven at 50 °C. The glass substrate was vertically soaked into the as-prepared sols for 2 min, and then the substrate was pulled out with the constant speed of 60 cm/min for 6 times. The thickness of TiO₂ and WO₃-TiO₂ films was ~130 nm. The films were coated on both sides of the glass substrate. After coating, the substrate was heated at 400 °C to promote the formation of crystalline WO₃-TiO₂.

Characterization

X-ray diffraction (XRD)

The crystalline structure of the as-prepared TiO₂ and WO₃-TiO₂ was performed using Siemens D500 powder diffractometer using CuK_{α1} radiation ($\lambda = 1.5405 \text{ \AA}$) at a voltage and current of 40 kV and 40 mA, respectively. The scanning range of 2θ was 20°–80° at a rate of 0.05°/min. The XRD sample was prepared by drying the TiO₂ or WO₃-TiO₂ sol at 100 °C for 2 day to obtain the powder sample and the sample was calcined at 400 °C for 3 h.

Scanning electron microscopy (SEM)

The morphology and thickness of films were observed by Hitachi-3000 with tungsten lamp at acceleration voltage of 10 kV and emission current of 81,000 nA. The SEM sample was prepared by cutting the coated glass substrate into 0.5 cm×0.5 cm pieces with diamond knife first and then coated with platinum to increase its conductivity.

Transmission electron microscopy (TEM) and high-resolution electron microscopy (HRTEM)

The morphologies of TiO₂ and WO₃-TiO₂ sols were observed by TEM (JEM-2000 EX II) operated at 160 kV or 200 kV and HRTEM (JEOL JEM-2100) operated at 200 kV. The TEM sample was prepared by dipping the carbon-coated copper grid (200 meshes) (Ted Pella) into the as-prepared sols for 3 times. The chemical composition of the sample was determined by energy-dispersive X-ray spectroscopy (EDS) attached on HRTEM using silicon detector.

X-ray photoelectron spectroscopy (XPS)

The XPS spectra were recorded with a Thermo VG Scientific Sigma Prob spectrometer. The XPS spectra were collected using Al K_α radiation at a voltage and current of 20 kV and 30 mA, respectively. The base pressure in the analyzing chamber was maintained in the order of 10^{−9} torr. The spectrometer was operated at 23.5 eV pass energy, and the binding energy was corrected by contaminant

carbon ($C_{1s} = 284.6$ eV) in order to facilitate the comparisons of the values among the catalysts and the standard compounds. Peak fitting was done by using XPSPEAK 4.1 with Shirley background and 30:70 Lorentzian/Gaussian convolution product shapes.

Photocatalytic reaction test

For the photocatalytic reaction test, 50 ml 10 ppm methylene blue solution was loaded into a quartz reactor. The glass substrate that was coated with TiO₂ or WO₃-TiO₂ film was then loaded into the reactor. The reactor was in the dark overnight to reach saturation of adsorption of methylene blue (MB) in the catalyst [48–53]. The photocatalytic reaction under UV light was then started. The UV light source was 20 W UVC lamp (wavelength = 254 nm). The concentration of MB was determined by UV–visible spectrophotometer (Cary 300 Bio). The detailed experimental procedure was reported in the previous literature [48–53].

Results and discussion

Characteristics of TiO₂ and WO₃-TiO₂ Sols

The as-prepared TiO₂ and WO₃-TiO₂ sols were synthesized with peroxo sol–gel method. The TiO₂ sol was light yellow transparent sol containing TiO₂ nanoparticles dispersed in water. The yellow color was due to the presence of small amount of titanium peroxide [48]. As the amount of H₂O₂ in preparation decreased, the color became lighter. The pH values of TiO₂ and WO₃-TiO₂ sols are listed in Table 1. The pH value of TiO₂ sol was 8.7. With increase in the heating time, the pH value of TiO₂ sol increased, due to the decrease of the amount of H₂O₂ in heating process. Table 1 shows that adding WO₃ to TiO₂ sol decreased the pH value slightly to be less basic, since the tungsten precursor was acidic. It was not able to synthesize stable WO₃-TiO₂ sol by peroxo sol–gel method if WO₃ content was greater than 4 wt.%.

Table 1 The pH values of the WO₃-TiO₂ as-prepared sols

Sample	pH value
TiO ₂	8.78
WT(0.5)	8.72
WT(1)	8.68
WT(2)	8.63
WT(4)	8.12

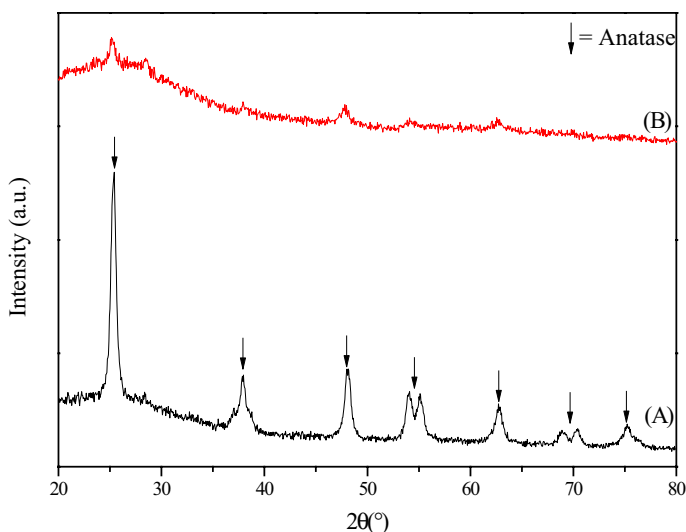


Fig. 2 XRD patterns of **a** TiO_2 nanoparticles obtained from the as-prepared TiO_2 sol and calcined at 400°C for 30 min and **b** the as-prepared TiO_2 nanoparticles without calcination

XRD

The as-prepared TiO_2 and $\text{WO}_3\text{-TiO}_2$ sols were heated at 100°C for 2 days to get powder samples. The XRD patterns are shown in Figs. 2. It shows the anatase TiO_2 diffraction peaks located at $2\theta = 25.4102^{\circ}$, 37.9658° , 48.1227° , 62.7199° and 75.2245° corresponding to the phase of (101), (004), (200), (204), and (215), respectively [5–8, 10–15, 48–53]. The as-prepared TiO_2 had low intensity peaks for anatase, as shown in Fig. 2b, because the TiO_2 crystallite size was very small. Figure 3 shows the XRD patterns of $\text{WO}_3\text{-TiO}_2$ samples. The diffraction peaks of these patterns are consistent with the characteristic peaks of anatase TiO_2 and did not show any diffraction peak of WO_3 , inferring WO_3 crystal was too small to detect. The characteristic peaks of $\text{WO}_3\cdot\text{H}_2\text{O}$ are at $2\theta = 25.7164^{\circ}$, 35.1076° and 52.7672° , respectively. Pan and Lee [16] reported that WO_3 was highly dispersed in the bulk phase of TiO_2 particles and WO_3 was not formed. Our results are in accord.

SEM

The structure of TiO_2 and $\text{WO}_3\text{-TiO}_2$ films was examined by SEM. The top-view surface structure and cross-sectional view of the as-prepared thin film are shown in Fig. 4. Each sample had very uniform and smooth surface of film on the top of the substrate, indicating that dip coating is a good way to prepare the thin film. The particle size of pure TiO_2 was smaller than those of $\text{WO}_3\text{-TiO}_2$ samples.

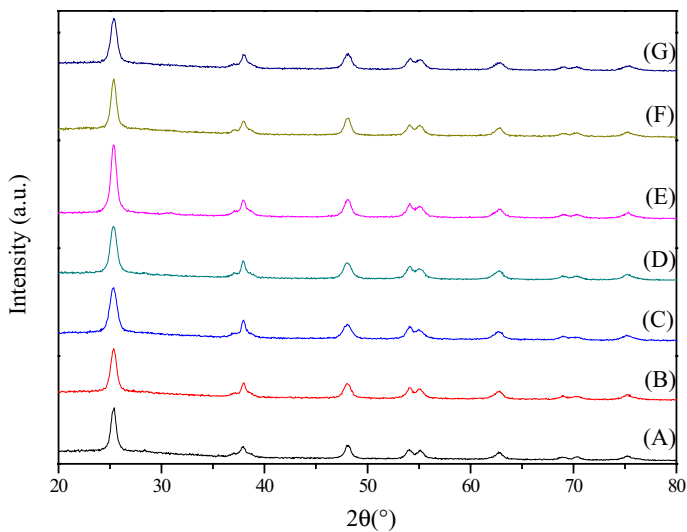


Fig. 3 XRD patterns of **a** TiO_2 calcined by 400°C , **b** WT(0.5), **c** WT(1), **d** WT(1.5), **e** WT(2), **f** WT(3), **g** WT(4)

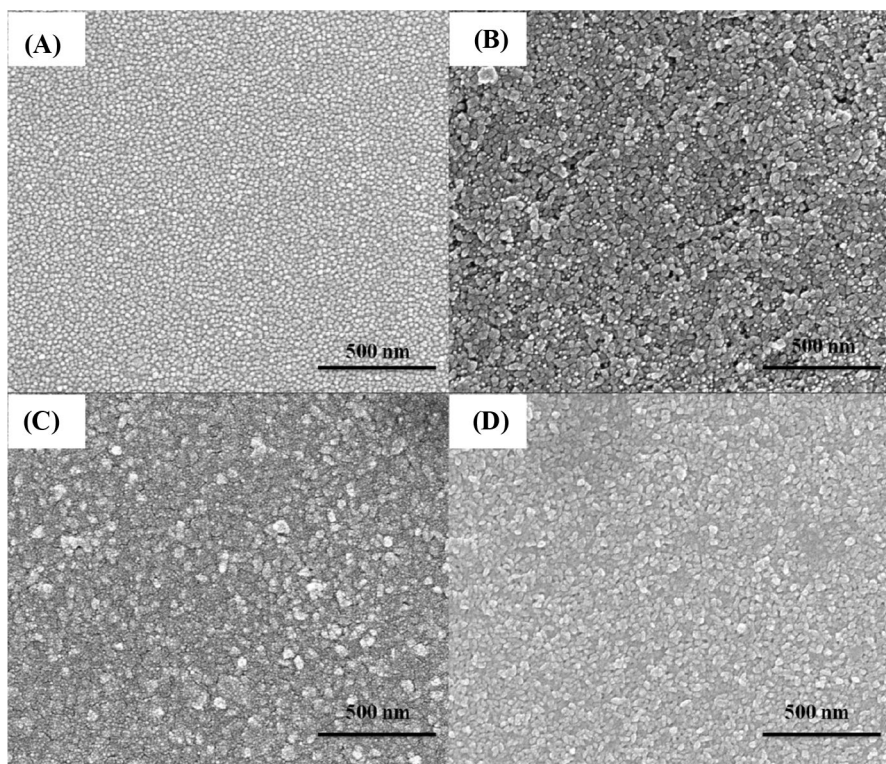


Fig. 4 Top view of the surface of **a** TiO_2 film, **b** WT(0.5) film, **c** WT(1) film, **d** WT(2) film

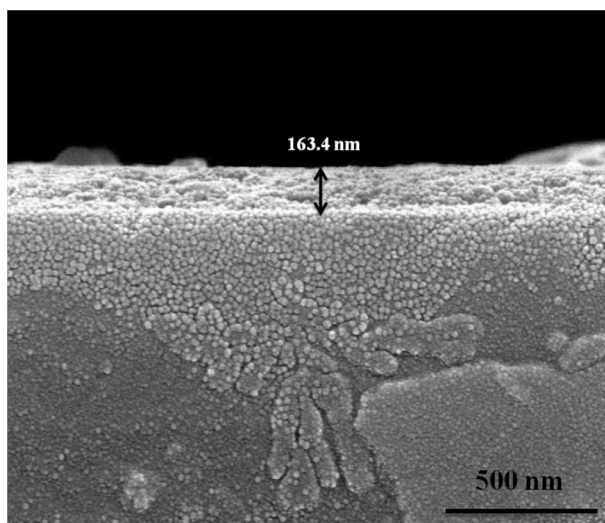


Fig. 5 Cross-sectional image of WO₃-TiO₂ film

Adding WO₃ to TiO₂ created rough surface which could enhance the adsorption of dye and increased surface area. This is beneficial for the photocatalytic activity as shown in the latter section. The typical cross-sectional view of WO₃-TiO₂ film is shown in Fig. 5. The film thickness of the WO₃-TiO₂ film was 163.4 nm. Since WO₃-TiO₂ formed anatase crystal in sol, no annealing is needed after coating on glass. In addition, WO₃-TiO₂ strongly sticks on the glass with 3H hardness.

TEM and HRTEM

The morphology of the as-prepared TiO₂ and WO₃-TiO₂ sols was analyzed by TEM and HRTEM. HRTEM image in Fig. 6d shows that the TiO₂ particles were rhombus shaped with the major axis and minor axis of 30–77 nm and 15–31 nm, respectively. The selected area electron diffraction (SAED) pattern confirms that TiO₂ nanoparticles were anatase, as indicated by the plane of (101), (103) and (211) [6, 48–53]. The lattice space of 0.395 nm corresponding to the (101) anatase plane is observed in Fig. 6c. Figure 7 shows the morphologies and particle sizes of the as-prepared WO₃-TiO₂. Compared with pure TiO₂ sol, the particle size of WO₃-TiO₂ was a little smaller than that of TiO₂. They also show rhombus shape.

In order to confirm whether WO₃ particle was dispersed in TiO₂ sol or not, WO₃ sample was prepared. Figure 8c shows that the shape of WO₃ was spherical-like and its average particle size was ~10 nm, which was smaller than that of TiO₂ particle. The WO₃-TiO₂ sample was also examined by EDS as shown in Fig. 8b. None of the particles were WO₃. One can conclude that WO₃ was incorporated into the structure of TiO₂ and no WO₃ particles were formed in this study, providing that the concentration of WO₃ was low. In conclusion, one has successfully developed a method to prepare WO₃-TiO₂ sol by peroxo sol–gel method.

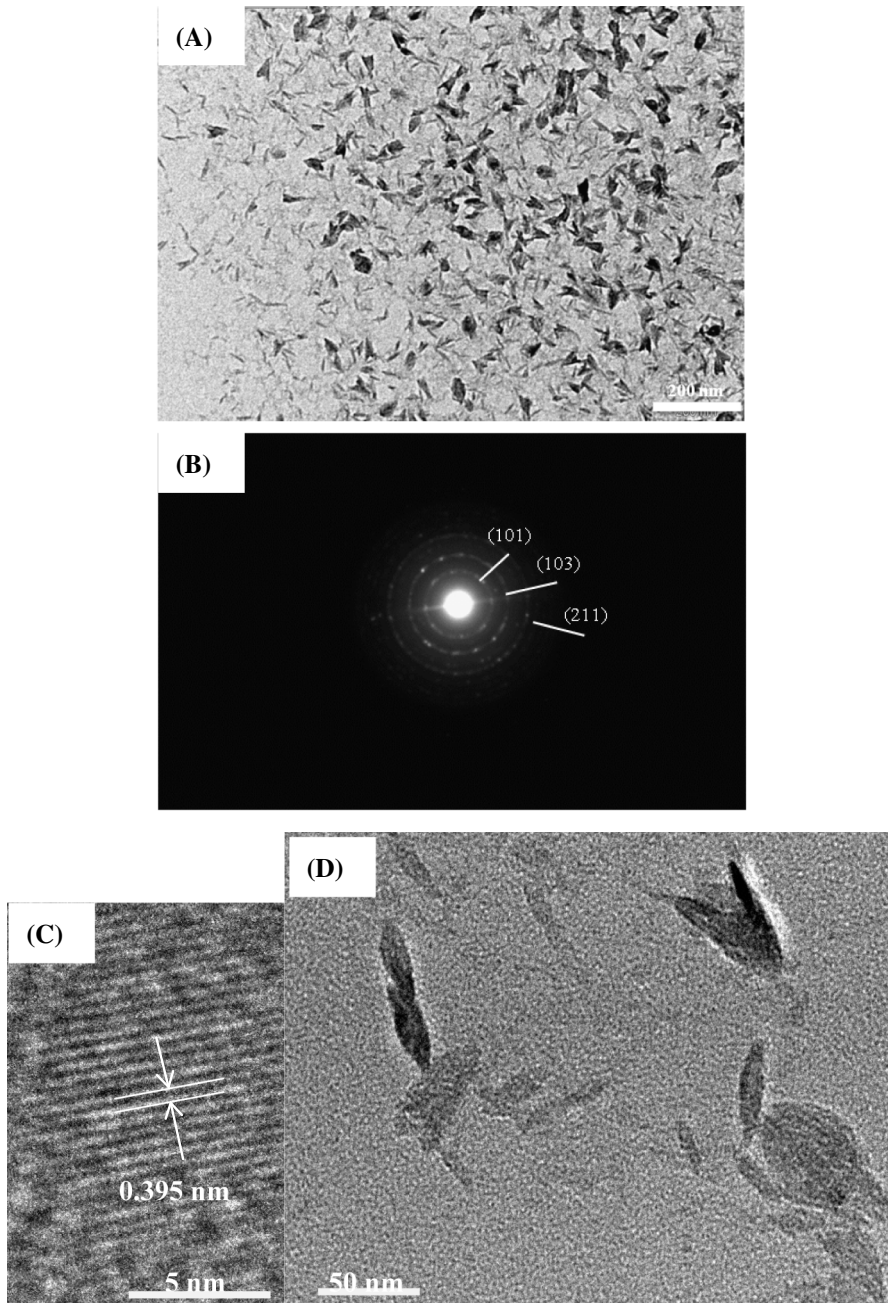


Fig. 6 **a** TEM image of TiO_2 , **b** The SAED pattern of TiO_2 , **c** the lattice space of TiO_2 from HRTEM, **d** HRTEM image of TiO_2

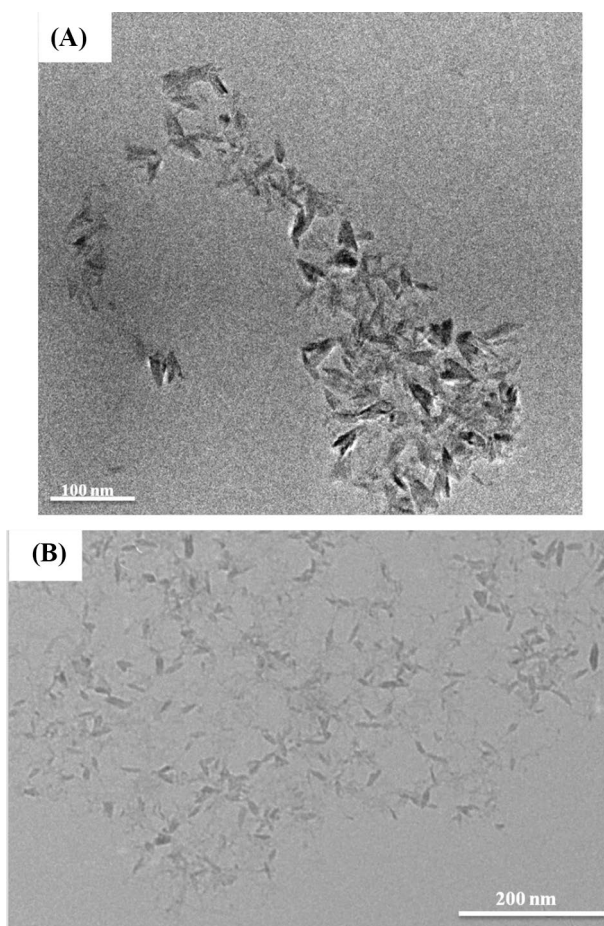


Fig. 7 TEM image of **a** WT(0.5) sol, **b** WT(4) sol

XPS

XPS analysis was performed to investigate the electronic state of each element of the sample. Based on the literature [45–50], the binding energy of $\text{Ti}^{4+} 2p_{3/2}$ and $\text{Ti}^{4+} 2p_{1/2}$ is centered at 458.6 eV and 464.4 eV, while the binding energy of $\text{Ti}^{3+} 2p_{3/2}$ and $\text{Ti}^{3+} 2p_{1/2}$ is centered at 457.7 eV and 463.5 eV [51–53]. The spectra of Ti 2p region of all samples are shown in Fig. 9. The contents of Ti^{4+} and Ti^{3+} are listed in Table 3. All samples showed large amount of Ti^{4+} and small amount of Ti^{3+} . WO_3 - TiO_2 samples had higher concentrations of Ti^{3+} than pure TiO_2 . WO_3 was incorporated into the surface structure of TiO_2 and modified the electronic state of Ti. Ti 2p (Ti^{4+}) of the WT(4) was observed at lower binding energy region than the Ti 2p (Ti^{3+}) of other 3 samples as shown in Fig. 9, possibly because this sample had higher content of WO_3 than the other 3 samples.

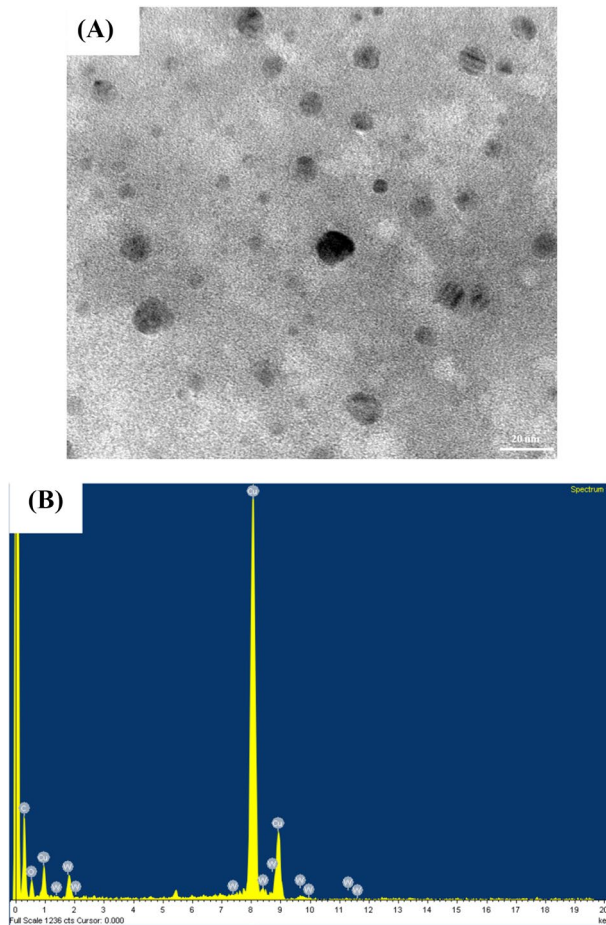


Fig. 8 **a** TEM image of WO₃, **b** EDS analysis of WO₃ particle

Some WO₃ had big particles and was not incorporated into surface structure of TiO₂. Further research is needed to address this difference.

Figure 10 shows the O 1s spectra of various samples. The spectra were deconvoluted to five peaks, i.e., 532.1 eV corresponding to oxygen in TiO₂ surface adsorption of OH[−], 529.9 eV corresponding to oxygen in TiO₂ lattice, 529.2 eV corresponding to oxygen in Ti–O–Ti bond, 530.2 eV corresponding to oxygen in TiO₂ surface adsorption of H₂O, 530.6 eV corresponding to oxygen in WO₃ lattice. The percentages of O^{2−} and OH[−] are listed in Table 3. The presence of OH[−] and O^{2−} species on the samples infers that they can become captives of photogenerated electron–hole pairs directly or indirectly to suppress the recombination of the photogenerated electron–hole pairs [46–53]. WT(4) sample had a lower contents of OH[−] and O^{2−} species, compared to other samples.

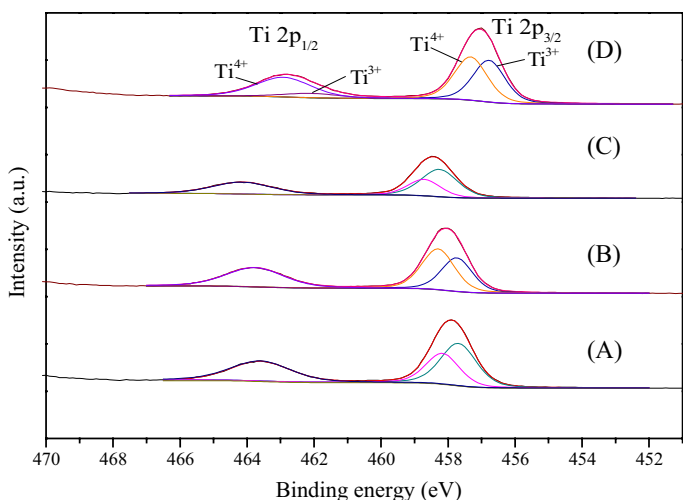


Fig. 9 Ti 2p XPS spectra of **a** WT(0.5) film, **b** WT(1) film, **c** WT(2) film and **d** WT(4) film

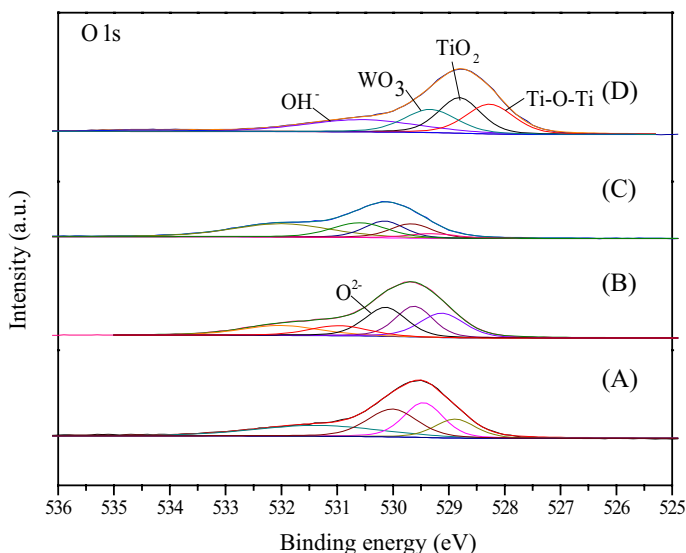


Fig. 10 O 1s XPS spectra of **a** WT(0.5) film, **b** WT(1) film, **c** WT(2) film and **d** WT(4) film

The XPS spectra of W 4f are shown in Fig. 11. It shows four peaks, because of W 4f_{7/2} and W 4f_{5/2} transition with different oxidation states of W atoms. The main peaks, having a W 4f_{5/2} at 37.8 eV and a W 4f_{7/2} at 35.7 eV, are attributed to the W atoms in 6+ oxidation state. The other oxidation state in W atoms is 5+ oxidation state with a W 4f_{5/2} at 34.6 eV and W 4f_{7/2} at 36.7 eV peaks [10–12]. The binding energy of W 4f in WT(4) sample had lower binding energy than the other 3 samples

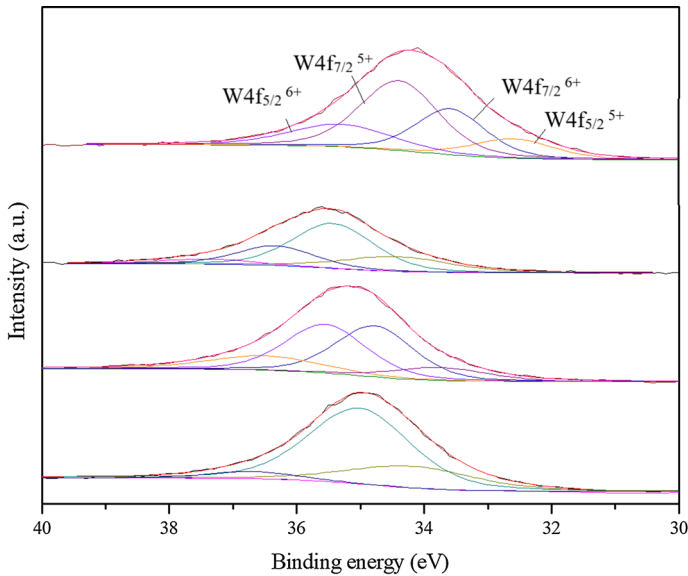


Fig. 11 W 4f XPS spectra of **a** WT(0.5), **b** WT(1), **c** WT(2) and **d** WT(4)

as shown in Fig. 11. The results are in accordance with the results of Ti 2p spectra. This is possibly because this sample had higher content of WO₃ than the other 3 samples. Some WO₃ had big particles and was not incorporated into surface structure of TiO₂. Further research is needed to address this difference (Table 2).

Photocatalytic destruction of methylene blue

The photocatalytic activities of TiO₂ and WO₃-TiO₂ thin films were tested by the photocatalytic destruction of MB. The saturation adsorption of MB in various samples is shown in Table 4. The results show that adding WO₃ in TiO₂ increased adsorption capacity of MB, because it had rougher surface than the undoped one.

The photocatalytic activities of the as-prepared TiO₂ and WO₃-TiO₂ films are shown in Figs. 12. The highest photocatalytic activities of film were WT(4) and WT(4) with the rate constant of 0.5138 h⁻¹, as obtained by plotting ln(C₀/C) against irradiation time corresponding to first-order reaction. The rate constants are listed in Table 5. It indicates that doping suitable amount of WO₃ in TiO₂ could increase the photocatalytic activity. The optimal weight ratio of WO₃/TiO₂ was 2/100. The WO₃-modified TiO₂ samples existed in Ti⁴⁺, Ti³⁺, W⁶⁺ and W⁵⁺ chemical states. Ti³⁺ and W⁵⁺ can gather the photogenerated holes from conduction band of TiO₂; however, Ti⁴⁺ and W⁶⁺ can capture the photogenerated electrons gathered in the lower conduction band of WO₃. This can effectively enhance the separation of photogenerated electron-hole pairs and increase the photocatalytic activity. It was not able to synthesize stable WO₃-TiO₂ sol by peroxo sol-gel method if WO₃ content was greater than 4 wt.%.

Table 2 Binding energies (eV) of various species

Sample	W		Ti				O					
	$4f_{5/2}$		$4f_{7/2}$		$2p_{3/2}$		$1s$		Ti-O-Ti	O ²⁻	WO ₃	
	6 +	5 +	6 +	5 +	3 +	4 +	3 +	4 +				
TiO ₂	–	–	–	–	456.7	461.8	463.6	–	530.0	527.9	528.5	–
WT(0.5)	36.5	35	35.0	36.7	457.8	458.2	463.6	463.7	531.3	529.4	528.9	530.0
WT(1)	35.6	34.8	35.0	35.9	457.8	458.2	463.6	463.7	532.0	529.6	529.1	530.1
WT(2)	35.6	34.2	35.0	35.8	457.8	458.3	463.6	463.7	531.6	529.7	529.2	530.2
WT(4)	34.6	33.8	34.2	32.5	456.8	457.2	463.0	462.8	531.3	529.5	529.0	530.0

Table 3 Concentrations of each chemical state of Ti, O and W by XPS analysis

Sample	W		Ti		O				
	W ⁶⁺	W ⁵⁺	Ti ⁴⁺	Ti ³⁺	OH ⁻	TiO ₂	Ti–O–Ti	O ²⁻	WO ₃
TiO ₂	–	–	7.58	92.42	31.76	–	29.80	38.44	–
WT(0.5)	70.01	29.99	29.02	70.97	27.72	28.02	15.78	0	28.48
WT(1)	52.12	47.88	70.12	29.89	16.05	23.80	22.66	25.27	12.23
WT(2)	56.72	43.28	55.25	44.76	35.69	18.51	16.81	6.44	22.56
WT(4)	51.25	48.75	61.36	38.65	24.34	26.44	24.99	2.66	21.57

Table 4 The saturation adsorption of methylene blue solution in the dark

Sample	MB concentration adsorbed by sample (%)
TiO ₂	8.840
WT(0.5)	9.579
WT(1)	16.191
WT(2)	12.686
WT(4)	13.926

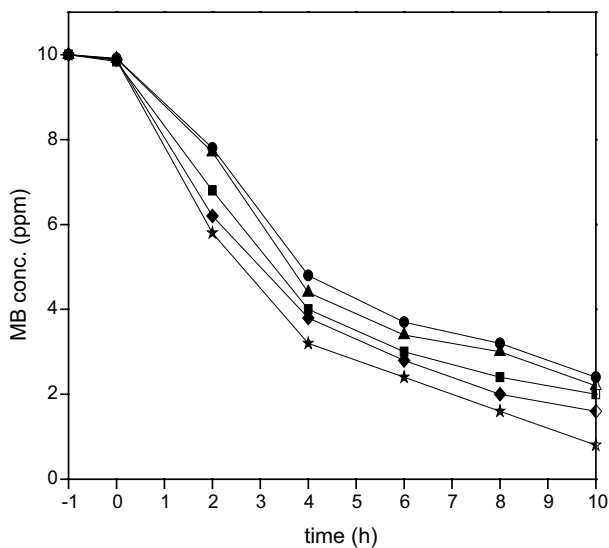
**Fig. 12** Photocatalytic degradation of methylene blue aqueous solution. Black circle TiO₂; black triangle WT(0.5); black square WT(1); black diamond WT(2); black star WT(4)

Table 5 Rate constant of reaction of MB destruction from pseudo-first-order kinetic

Catalyst	Rate constant (h^{-1})
TiO ₂	0.3728
WT(0.5)	0.3823
WT(1)	0.4108
WT(2)	0.4273
WT(4)	0.5138

Conclusion

The results of this study are summarized as follows:

1. A series of WO₃-modified TiO₂ sols with various WO₃ contents were synthesized by peroxo sol–gel method. The WO₃-TiO₂ sols were light yellow in color. The pH values of the as-prepared sols were neutral to weak basic. These sols were very stable even after 2 years in stock. The sols can be used to coat on glass substrate.
2. The XRD patterns and the SAED patterns indicated that the phase of TiO₂ was anatase. There were no WO₃ peaks, and particles appeared in the WO₃-modified TiO₂ sol. The particles were rhombus shaped with the major axis and minor axis of 30–77 nm and 15–31 nm, respectively. WO₃ was incorporated into the surface structure of TiO₂ and modified the electronic state of Ti.
3. The SEM results showed that the film coated onto glass substrate was very uniform and the film thickness was ~ 160 nm.
4. The XPS results exhibited that W existed as 5+ and 6+ oxidation states and Ti existed in Ti³⁺ and Ti⁴⁺. These four chemical states play a role of gathering the photogenerated holes and capturing the photogenerated electrons in the lower conduction band of WO₃, respectively. This can effectively enhance the separation rate of photogenerated electron–hole pairs and increase the photoactivity.
5. The optimal doping ratio of TiO₂/WO₃ was 100:4. It had high photoactivity under UV light illumination to degrade organic dye, because it had high OH and O²⁻ group contents.

Acknowledgements This research was supported by Ministry of Science and Technology, Taiwan.

References

1. M. Dahl, Y. Liu, Y. Yin, *Chem. Rev.* **114**, 9853 (2014)
2. M.G. Ju, G. Sun, J. Wang, Q. Meng, W.Z. Liang, *ACS Appl. Mater. Interfaces* **6**, 12885 (2014)
3. H.C. Tseng, Y.W. Chen, *Mod. Res. Catal.* **9**, 1 (2020)
4. M. Rebeca, S. Joice, T.M. David, P. Wilson, *J. Phys. Chem. C* **123**, 27448 (2019)
5. F. Riboni, L.G. Bettini, D.W. Bahnemann, E. Selli, *Catal. Today* **209**, 28 (2013)
6. K. Ueyama, T. Hatta, A. Okemoto, K. Taniya, Y. Ichihashi, S. Nishiyama, *Res. Chem. Intermed.* **44**, 629 (2018)
7. N. Negishi, K. Takeuchi, *Res. Chem. Intermed.* **29**, 861 (2003)
8. S. Bellatreche, A. Hasnaoui, B. Boukoussa, J. Garcia-Aguilar, A. Berenguer-Murcia, D. Cazorla-Amoros, A. Bengueddach, *Res. Chem. Intermed.* **42**, 8039 (2016)
9. R.M. Mohamed, A.A. El-Midany, I. Othman, *Res. Chem. Intermed.* **34**, 629 (2008)

10. K.Y. Song, M.K. Park, Y.T. Kwon, H.W. Lee, W.J. Chung, W.I. Lee, *Chem. Mater.* **13**, 2349 (2001)
11. S. Meng, W. Sun, S. Zhang, X. Zheng, X. Fu, S. Chen, *J. Phys. Chem. C* **122**, 26326 (2018)
12. V. Štengl, J. Velická, M. Maříková, T.M. Grygar, A.C.S. Appl. Mater. Interfaces **3**, 4014 (2011)
13. V. Luca, M.G. Blackford, K.S. Finnie, P.J. Evans, M. James, M.J. Lindsay, M. Skyllas-Kazacos, P.R.F. Barnes, *J. Phys. Chem. C* **111**, 18479 (2007)
14. B. Gao, Y. Ma, Y. Cao, W. Yang, J. Yao, *J. Phys. Chem. B* **110**, 14391 (2006)
15. G. Ren, Y. Gao, J. Yin, A. Xing, H. Liu, *J. Chem. Soc. Pak.* **33**, 666 (2011)
16. J.H. Pan, W.I. Lee, *Chem. Mater.* **18**, 847 (2006)
17. F. Huguenin, V. Zucolotto, A.J.F. Carvalho, E.R. Gonzalez, O.N. Oliveira, *Chem. Mater.* **17**, 6739 (2005)
18. Y. He, Z. Wu, L. Fu, C. Li, Y. Miao, L. Cao, H. Fan, B. Zou, *Chem. Mater.* **15**, 4039 (2003)
19. M. Miyachi, A. Nakajima, T. Watanabe, K. Hashimoto, *Chem. Mater.* **14**, 4714 (2002)
20. G.M. Kumar, P. Ilanchezhian, C. Siva, A. Madhankumar, T.W. Kang, D.Y. Kim, *Appl. Surf. Sci.* **496**, 143652 (2019)
21. F. Azeez, E. Al-Hetlani, M. Arafa, Y. Abdelmonem, A.A. Nazeer, M.O. Amin, M. Madkour, *Sci. Rep.* **8**, 7104 (2018)
22. N. Yoshida, T. Watanabe, *Handbook of Sol-Gel Science and Technology* (2018) 2695.
23. B. Sarkar, A.V. Daware, P. Gupta, K.K. Krishnani, S. Baruah, S. Bhattacharjee, *Environ. Sci. Pollut. Research* **24**, 25775 (2017)
24. W.G. Wang, L. Zhu, Y.Y. Weng, W. Dong, *Chin. Phys. Lett.* **34**, 028201 (2017)
25. J. Mioduska, A. Zielińska-Jurek, M. Janczarek, J. Hupka, *J. Nanomater.* (2016) 18.
26. Oh JY, Lee BR, Kim HM, Lee CH (2015) *J. Korean Inst. Electr. Electron. Mater. Eng.* **28**: 715.
27. Y. Li, Z. Liu, L. Zhao, T. Cui, B. Wang, K. Guo, J. Han, *Electrochim. Acta* **173**, 117 (2015)
28. H.M. Kim, D. Kim, B. Kim, *Surf. Coat. Technol.* **271**, 18 (2015)
29. S. Liu, J. Huang, L. Cao, J. Li, H. Ouyang, X. Tao, C. Liu, *Mater. Sci. Semicond. Process.* **25**, 106 (2014)
30. S. Prabhu, A. Nithya, S.C. Mohan, K. Jothivenkatachalam, *Mater. Sci. Forum* **781**, 63 (2014)
31. Y. Li, P.C. Hsu, S.M. Chen, *Sensors and Actuators B: Chem.* **174**, 427 (2012)
32. R.Q. Cabrera, E.R. Latimer, A. Kafizas, C.S. Blackman, C.J. Carmalt, I.P. Parkin, *J. Photochem. Photobiol. A Chem.* **239**, 60 (2012)
33. E. Grabowska, J.W. Sobczak, M. Gazda, A. Zaleska, *Appl. Catal. B Environ.* **117–118**, 351 (2012)
34. Y. Zhu, X. Su, C. Yang, X. Gao, F. Xiao, J. Wang, *J. Mater. Chem.* **22**, 13914 (2012)
35. M.R. Bayati, F. Golestani-Fard, A.Z. Moshfegh, R. Molaei, *Mater. Chem. Phys.* **128**, 427 (2011)
36. S.A.K. Leghari, S. Sajjad, F. Chen, J. Zhang, *Chem. Eng. J.* **166**, 906 (2011)
37. D. Su, J. Wang, Y. Tang, C. Liu, L. Liu, X. Han, *Chem. Commun.* **47**, 4231 (2011)
38. Y. Murakami, I. Ohta, T. Hirakawa, Y. Nosaka, *Chem. Phys. Lett.* **493**, 292 (2010)
39. A.K.L. Sajjad, S. Shamaila, B. Tian, F. Chen, J. Zhang, *Appl. Catal. B Environ.* **91**, 397 (2009)
40. S. Biswas, M.F. Hossain, M. Shahjahan, K. Takahashi, T. Takahashi, A. Fujishima, *J. Vacuum Sci. Technol. A: Vacuum, Surfaces, and Films* **27** (2009) 880.
41. D.S. Kim, J.H. Yang, S. Balaji, H.J. Cho, M.K. Kim, D.U. Kang, Y. Djaoued, Y.U. Kwon, *CrystEngComm* **11**, 1621 (2009)
42. J. Li, J. Xu, W.L. Dai, H. Li, K. Fan, *Appl. Catal. B Environ.* **82**, 233 (2008)
43. K.K. Akurati, A. Vital, J.P. Dellemann, K. Michalow, T. Graule, D. Ferri, A. Baiker, *Appl. Catal. B Environ.* **79**, 53 (2008)
44. D. Ke, H. Liu, T. Peng, X. Liu, K. Dai, *Mater. Lett.* **62**, 447 (2008)
45. S.Y. Chai, Y.J. Kim, W.I. Lee, *J. Electroceramics* **17**, 909 (2006)
46. S. Wang, X. Zhang, G. Cheng, X. Jiang, Y. Li, Y. Huang, Z. Du, *Chem. Phys. Lett.* **405**, 63 (2005)
47. Y.W. Chen, J.Y. Chang, B. Moongraksathum, *J. Taiwan Inst. Chem. Eng.* **52**, 140 (2015)
48. B. Moongraksathum, Y.W. Chen, *J. Sol-Gel Sci. Technol.* **77**, 288 (2016)
49. A. Rismanchian, Y.W. Chen, S.S.C. Chuang, *Catal. Today* **264**, 16 (2016)
50. B. Moongraksathum, P.T. Hsu, Y.W. Chen, *J. Sol-Gel Sci. Technol.* **78**, 647 (2016)
51. B. Moongraksathum, Y.W. Chen, *J. Sol-Gel Sci. Technol.* **82**, 772 (2017)
52. B. Moongraksathum, Y.W. Chen, *Catal. Today* **310**, 69 (2018)
53. B. Moongraksathum, J.Y. Shang, Y.W. Chen, *Catalysts* **8**, 352 (2018)
54. B. Moongraksathum, M.Y. Chien, Y.W. Chen, *J. Nanosci. Nanotechnol.* **19**, 1 (2019)